Journal of Hydrology 675 (2026) 135535

Contents lists available at ScienceDirect

Journal of Hydrology

journal homepage: www.elsevier.com/locate/jhydrol

Research papers

Scaling relationships between catchment area and peak discharge across the Fitzroy Basin, eastern Australia

Jasmine B.D. Jaffrés [a,b,*], Chris Cuff [a], Cecily E. Rasmussen [a]

[a] C&R Consulting, 188 Ross River Rd, Townsville, Australia
[b] College of Science and Engineering, James Cook University, Townsville, Australia

ARTICLE INFO

This manuscript was handled by Dr Y Huang, Editor-in-Chief

Keywords:
Specific discharge
Catchment area
Fitzroy Basin
Extreme flow events
Stream gauge analysis
Flow–area scaling

ABSTRACT

Specific discharge – the flow rate per unit catchment area – highlights the spatial variability of rainfall–runoff events. These events rarely affect entire catchments uniformly, particularly in large river systems such as the Fitzroy Basin in eastern Australia. Using peak historical flow rates from 136 stream gauges, this study evaluates log–log scaling relationships between catchment area and specific discharge across the entire basin and nine major, nested subcatchments. The site-specific historical peaks across such a large and hydrologically diverse basin are used to assess how scaling behaviour varies with operational record length, rainfall extent and subcatchment characteristics. Peak specific discharge exhibits a strong inverse relationship with catchment area, consistent with power-law scaling. However, this relationship is more robust for gauges with longer operational records. Short operational periods reduce the likelihood of capturing rare, high-magnitude flow events and can substantially weaken scaling regressions. The analysis identifies specific gauges that exert disproportionate influence on the fitted exponents, offering practical guidance for gauge selection in future scaling and flood-frequency studies. Accurate estimation of extreme flows is further complicated by highly complex, non-stationary riverbed cross-sections, with some floodplains spanning several kilometres, reducing the reliability of rating curves during major floods. Improved characterisation of peak specific discharge enhances the predictive capacity for extreme flow rates, particularly under projected increases in atmospheric moisture that are likely to amplify peak flows during extreme rainfall events.

1. Introduction

Power-law relationships between peak flow and catchment area arise naturally from scale-invariant runoff generation processes (Gupta and Waymire, 1998). However, real basins often deviate from idealised scaling because of climatic and geomorphological heterogeneity. The concept of flow–area scaling laws – describing the relationship between peak discharge (Q) and catchment area (A) – has been widely examined. Expressed as a power-law function ($Q \propto A^{\beta}$; e.g. Smith, 1992), this empirical framework has been applied internationally to understand runoff generation and flood magnitude across catchments. Reported scaling exponents (β) vary considerably between regions, reflecting differences in hydroclimatic regime, intrinsic catchment attributes and data resolution. Liu et al. (2017) tabulated β values and corresponding catchment sizes of earlier studies, with β = 0.52–0.85 and A = 0.00183–91,000 km^2. Along with catchment area, studies have differed in the streamflow metric used for scaling, ranging from typical or low-flow conditions to extreme flood events.

Additional complexity is illustrated by Galster (2007), who investigated annual mean and peak discharges over at least 60 years for five rivers in the contiguous United States and found non-stationarity of β at one site (the semi-arid Yellowstone River). Averaged over the full historical record per site, β ranged from 0.49 to 0.97 for peak annual discharge, with a narrower range for annual mean discharge (0.50–0.80).

More generally, evaluated catchments in previous studies tend to be small- to medium-sized, rather than large and heterogeneous. Large, hydrologically heterogeneous basins often exhibit scale-dependent flood behaviour (Blöschl and Sivapalan, 1995), with spatial variability in inundation patterns and hydrogeomorphological processes such as floodplain connectivity modulating peak flows (Costabile et al., 2024). Yet such evidence remains limited in many regions, including subtropical Australian systems, partly due to sparse gauging networks, short observational records and inconsistent definitions of flood peaks.

* Corresponding author at: C&R Consulting, 188 Ross River Rd, Townsville, Australia.
E-mail address: Jasmine@candrconsulting.com.au (J.B.D. Jaffrés).

https://doi.org/10.1016/j.jhydrol.2026.135535
Received 14 November 2025; Received in revised form 3 April 2026; Accepted 18 April 2026
Available online 19 April 2026

The magnitude of peak flows is constrained by intrinsic catchment characteristics such as subsurface permeability, topography and soil moisture, which influence flow behaviour (Jaffrés et al., 2021; Wasko et al., 2021) and thereby control flow attenuation. Topography is associated closely with streamflow flashiness (Kuentz et al., 2017). However, climate and weather – specifically spatiotemporal rainfall patterns – are the overarching regulators of extreme flow peaks and frequency. Robinson and Sivapalan (1997) identified five flow response regimes – from very fast responses driven by in-storm rainfall variability to very slow responses governed by seasonal controls – highlighting the spectrum of hydroclimatic influence on peak-flow generation.

This study addresses these issues by examining flow–area scaling in a climatically variable region where extreme rainfall events are modulated by both large-scale climate phenomena (e.g. El Niño–Southern Oscillation [ENSO]) and synoptic systems such as tropical cyclones (TCs), monsoon troughs and frontal systems (Higgins et al., 2022; Jaffrés et al., 2018; Risbey et al., 2009). By quantifying how peak flows scale with catchment area under diverse rainfall regimes, the work contributes to international understanding of scaling variability and provides evidence from a hydroclimatic context that remains underrepresented in global analyses.

The Fitzroy Basin – located in central eastern Queensland, Australia – plays a critical role in regional water security, agricultural productivity and ecological connectivity. Increasing land-use intensity and hydrological modification have altered runoff regimes and wetland conditions, with implications for water quality and ecosystem resilience. The basin is also a major source of freshwater, sediments and nutrients to the Great Barrier Reef lagoon (Lewis et al., 2015). Understanding the scaling relationship between catchment area and peak runoff yield is therefore important for predicting streamflow responses under changing climatic and land-use conditions, and for improving hydrological modelling in large, heterogeneous basins.

Unlike previous research, this study focuses on gauge-specific record flows, meaning that there is no event-based scaling or scaling over a fixed period (e.g. a year). Furthermore, specific discharge ($q = Q/A$) – rather than total discharge – was used to facilitate the comparison of nested subcatchments of disparate sizes and upstream areas. Specific discharge is widely used in hydrological studies, including in flow-duration analysis (Castellarin et al., 2004) and low-flow regionalisation (Laaha and Blöschl, 2006).

This study tests the hypothesis that peak specific discharge exhibits a consistent inverse power-law scaling relationship with catchment area across the Fitzroy Basin. The main objective is to determine this scaling relationship both basin-wide and across nine major subcatchments to assess regional variability. Three specific objectives are addressed: 1) assessing how operational record length among stream gauges influences scaling behaviour, 2) evaluating the role of hydroclimatic drivers in explaining subcatchment variability, and 3) examining the reliability of rating curves during extreme flows, including a sensitivity analysis of Manning's roughness coefficient (n_M).

2. Methods

2.1. Study area

The Fitzroy Basin in central eastern Queensland, Australia, is one of the country's largest catchments, covering approximately 143,000 km^2. The basin is comparable in size to Tajikistan and larger than Greece, making it the largest river system in eastern Australia and the primary freshwater contributor to the Great Barrier Reef. This largely rural basin encompasses diverse landscapes ranging from rugged highlands to extensive floodplains, resulting in complex hydrological behaviour, including variable flow regimes and seasonal extremes.

According to the modified Köppen–Geiger climate classification (Beck et al., 2018), most of the Fitzroy Basin area (~72%) is subtropical, dominated by a hot, arid steppe (BSh) climate. Temperate regions with hot summers and no dry season (Cfa) account for approximately 21% of the basin (Fig. 1; Table 1). The northeastern Connors Range is classified as temperate with dry winters and hot summers (Cwa, ~6%). The downstream Fitzroy River corridor includes a small tropical savannah component (Aw, ~1%), although Cfa is the dominant class in this lower basin region (Table S1).

Flows in the Fitzroy Basin are highly seasonal, with high-flow episodes occurring predominantly during austral summer (December–March; Webster and Ford, 2010). Many rivers and streams in the basin exhibit non-perennial flow regimes, with high interannual and seasonal variability reflecting rainfall distribution and catchment characteristics. This variability is often structured around the water year, with pronounced wet and dry seasons driven by large-scale climate phenomena such as ENSO, the Madden–Julian oscillation and the position of the monsoon trough. Notable flow events are typically generated by extreme rainfall over multiple subcatchments, often combined with antecedent wet conditions. Rainfall across the basin tends to peak in January or February, with August and September generally the driest months (Fig. 2). Accordingly, the regional water year is defined as September to August.

Spatial gradients in rainfall align closely with climate class. The driest regions are associated with the BSh zone, whereas the wettest areas correspond to Cwa, followed by Aw. The northern Connors River subcatchment within the Cwa climate class exhibits the highest median annual rainfall, as indicated by the Scientific Information for Land Owners (SILO; Jeffrey et al., 2001) grid point at 149.05°E and 21.75°S (1,005.7 mm; Table 2). This region is also strongly wet-season-dominated, with 74.1% of rainfall occurring between November and March. In contrast, the adjacent Isaac River subcatchment is substantially drier (551.1 mm at 148.05°E, 22.10°S, BSh zone; Fig. 2a). Table 2

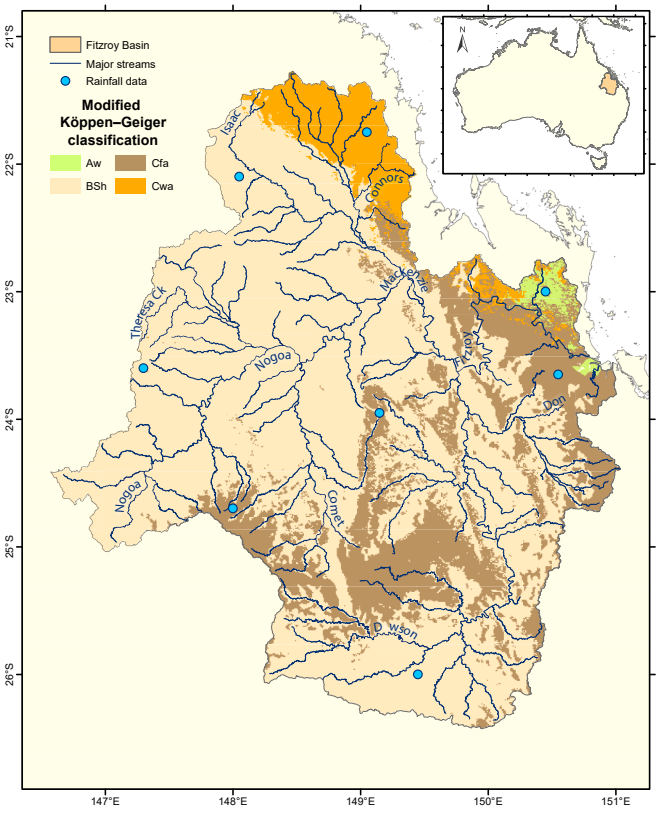

Fig. 1. Fitzroy Basin climate based on the modified Köppen–Geiger classification (adapted from Beck et al., 2018). Major stream networks and the eight locations for which rainfall data were obtained are also displayed (see Fig. 2 for rainfall patterns). The inset map shows the position of the Fitzroy Basin within Australia.

Table 1
Prevalence (percentage of total basin area) and description of Köppen–Geiger climate classes within the Fitzroy Basin.

Class	Basin area (%)	Description
Aw	0.97	Tropical savannah
BSh	72.21	Hot, arid steppe
Cfa	20.85	Temperate, hot summers without a dry season
Cwa	5.97	Temperate, dry winters and hot summers

summarises rainfall metrics, climate class, elevation and nearby subcatchments for all eight SILO points.

The lower Fitzroy Basin also receives relatively high annual rainfall, particularly within the Aw zone (883.4 mm at 150.45°E, 23.00°S). Rainfall is more evenly distributed seasonally compared with the Cwa example from the Connors River, with 67.3% occurring during the wet season (Fig. 2b, Table 2), although the seasonality remains distinct. Further inland, rainfall seasonality is weaker, with 62.0% attributed to the wet season in these drier areas. Near the coast, intense rainfall is commonly associated with atmospheric lows, including TCs, whereas inland regions predominantly receive rainfall from ex-TCs following inland trajectories and from localised thunderstorms. These spatial rainfall gradients – together with contrasting physiography across the basin – underpin hydrological connectivity among the major subcatchments.

To support basin-wide and subcatchment-scale analyses of extreme streamflow and specific discharge, the Fitzroy Basin and its stream gauges were subdivided into nine nested catchments based on hydrological connectivity (Fig. 3). The Connors River subcatchment lies in the northeast of the basin and merges with the Isaac River to its west, with both systems flowing southwards. In the western basin, the Nogoa River flows eastward, merging first with Theresa Creek and later with Crinum Creek, shortly before its confluence with the Comet River. The junction of the eastward-flowing Nogoa River and the northward-flowing Comet River marks the start of the Mackenzie River, which initially flows northeastwards before turning south after merging with the Isaac River.

The southern portion of the basin is dominated by the Dawson River, the most extensive subcatchment, which initially flows eastwards before adopting a northerly course. In its lower reaches, the Don River subcatchment joins the Dawson River from the east. Downstream of the confluence between the Dawson and Mackenzie rivers, the system becomes the Fitzroy River, which ultimately discharges into the Coral Sea.

2.2. Stream gauge data

Stream gauge metadata and discharge records (including operational period, upstream area A, and flow rate Q) were obtained from the Queensland Department of Natural Resources, Mines and Energy Water Monitoring Information Portal (WMIP; https://water-monitoring.information.qld.gov.au/). The complete archive of open and closed stations was downloaded in January 2025, with data coverage extending to early 2024. Cross-sections and monthly discharge volumes for selected gauges were also accessed from WMIP.

Of the 159 stations within the Fitzroy Basin, 17 were excluded because their catchment area (A) was unspecified, and six (6) because no non-zero flow rate (Q) was recorded. The remaining 136 gauges span all nine nested catchments. The spatial distribution and operational periods of these gauges are shown in Fig. 3.

Specific discharge was defined as $q = Q/A$. A log–log transformation of catchment area and specific discharge was applied to enable estimation of the area–discharge scaling exponent using linear regression:

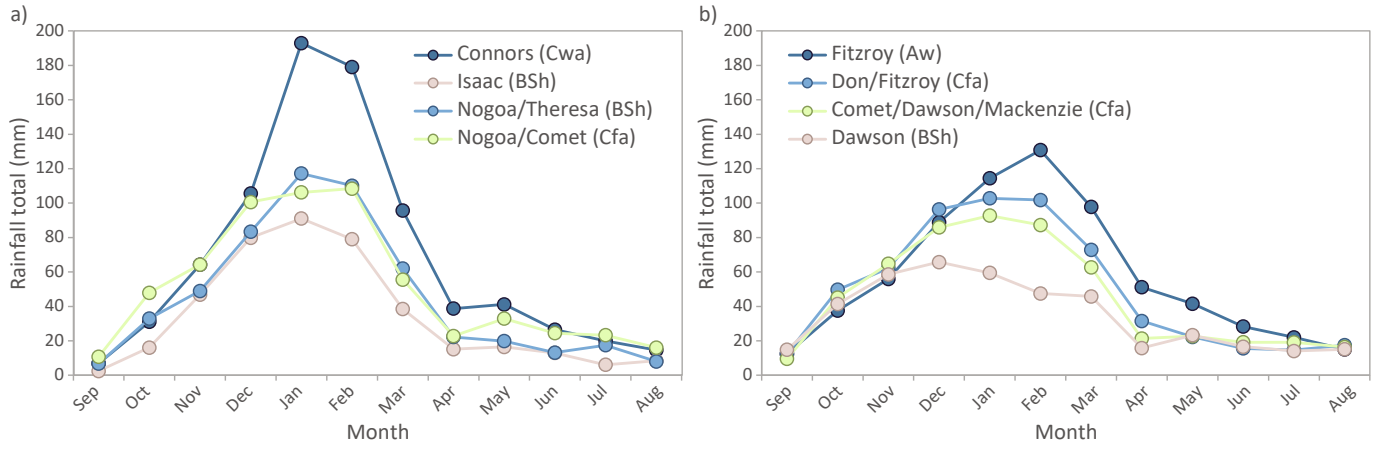

Fig. 2. Median monthly rainfall totals for water years within the Fitzroy Basin. Rainfall data from SILO (Scientific Information for Land Owners) are shown for locations in a) the north and west, and b) the east, centre and south of the basin. The legend identifies nearby subcatchments and the associated modified Köppen–Geiger climate class for each SILO point. The SILO points correspond to the locations listed in Table 2.

Table 2
Median rainfall (1950–2025) per water year (September–August) and wet season (November–March) for eight SILO (Scientific Information for Land Owners) grid points (Fig. 1). Corresponding Köppen–Geiger (K–G) climate classes, elevation and nearby subcatchments are also indicated.

Subcatchment[#]	K–G class	Elevation (m)	SILO (1950–2025 median) Longitude (°E)	Latitude (°S)	Water year (mm)	Wet season (mm)	Wet season (%)
Connors	Cwa	282	149.05	21.75	1,005.7	711.5	74.13
Isaac	BSh	244	148.05	22.10	551.1	391.4	70.96
Fitzroy	Aw	8	150.45	23.00	883.4	519.5	67.35
Nogoa/Theresa	BSh	484	147.30	23.60	743.4	454.3	68.28
Don/Fitzroy	Cfa	39	150.55	23.65	783.2	515.6	67.63
Comet/Dawson	Cfa	510	149.15	23.95	698.4	453.0	65.56
Dawson	BSh	239	149.45	26.00	530.9	335.4	61.99
Nogoa/Comet	Cfa	613	148.00	24.70	737.0	456.0	66.43

[#] Subcatchment names refer to areas in the vicinity of each SILO point rather than the exact grid location.

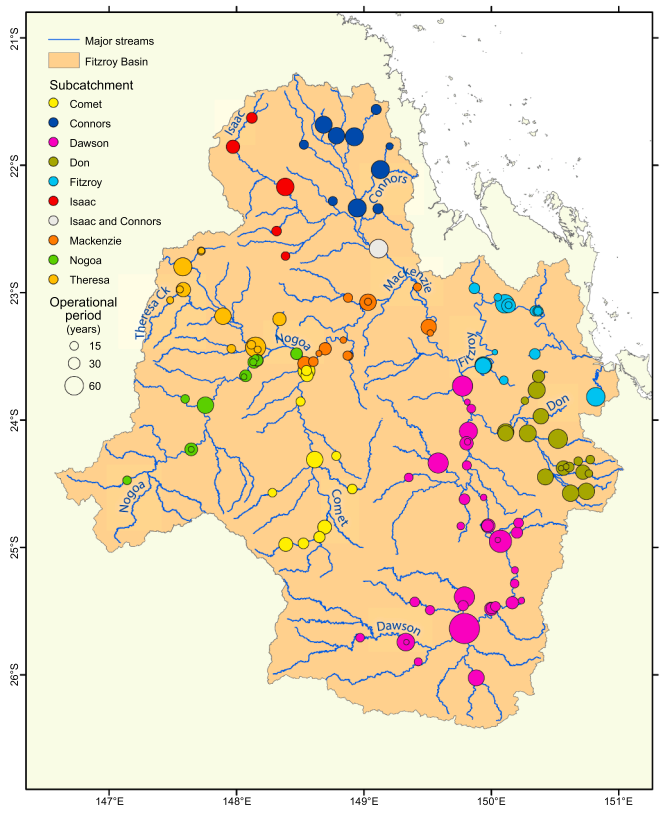

Fig. 3. Operational period (symbol size) of stream gauge stations within each subcatchment (symbol colour) of the Fitzroy Basin. The gauge data were obtained from the Water Monitoring Information Portal (WMIP).

$$A_{\log} = \log_{10}(A)$$

$$q_{\log} = \log_{10}(Q/A)$$

The relationship between specific discharge and catchment area was modelled as a power law:

$$q = kA^{\gamma},$$

with exponent γ estimated as the slope of the linear regression between $q_{\log}$ and $A_{\log}$. Because total discharge satisfies $Q = qA$, the corresponding scaling for total discharge and catchment area is $Q = kA^{\beta}$, with $\beta = \gamma + 1$.

The operational period for each gauge was defined as the number of years between the commence and cease dates in WMIP. For gauges still operating at the time of data access, the cease date was set to 1 January 2024.

2.3. Statistical methods

A regression analysis of $A_{\log}$ versus $q_{\log}$ was applied to the complete dataset and then repeated for each of the nine nested catchments. All gauges were first included in the full-basin analysis, then assigned to their respective subcatchments for nested analyses. Gauge 130401A (Isaac River at Yatton) was the only gauge assigned to more than one subcatchment. Although located at the confluence of the Isaac and Connors rivers – and nominally associated with the Isaac River – local hydrological knowledge indicates that its discharge record is often more representative of the Connors River subcatchment. For this reason, its discharge series was used in the analyses for both subcatchments.

Although the regression was performed using specific discharge, the resulting exponent (γ) was converted to the equivalent total–discharge exponent ($\beta = \gamma + 1$), enabling direct comparison with the widely used Q–A scaling relationship.

The Pearson correlation coefficient (r) between $A_{\log}$ and $q_{\log}$ was calculated for the complete dataset ($n = 136$). The Fisher z-transformation and associated standard error (SE) were then applied to derive the confidence interval (CI):

$$z = 0.5 \times \ln\left(\frac{1+r}{1-r}\right)$$

$$\mathrm{SE} = \frac{1}{\sqrt{n-3}}$$

CI in z-space:

$$z \pm z_{\alpha/2} \times \mathrm{SE}$$

Back-transformation to r:

$$r = \frac{e^{2z}-1}{e^{2z}+1}$$

The site with the shortest operational period was then iteratively removed to assess sensitivity to record length, with the process of r and CI derivation repeated until the sample size dropped below $n = 4$.

To assess the potential effect of rating-curve uncertainty at extreme stages, a simple sensitivity analysis was applied to the two largest recorded events (130401A in 2017 and 130003A in 1954). Flow rate Q in open channels is given by Manning's equation:

$$Q = \frac{1}{n_{\mathrm{M}}} A_c R^{2/3} S^{1/2}$$

where A_c is the cross-sectional area, R is the hydraulic radius (calculated as A_c/P, where P is the wetted perimeter), and S is the slope of the energy grade line. Here, A_c, R and S are held constant and only n_{M} is varied, making Q directly proportional to $1/n_{\mathrm{M}}$.

Manning's roughness values for vegetated floodplains were taken from published guidance (Arcement and Schneider, 1989). A plausible range of 0.035–0.090 was adopted to bracket seasonal and event-scale variability in floodplain vegetation and surface conditions, and a representative value of $n_{\mathrm{M}} = 0.06$ (the central value of the adopted range) was assumed for the WMIP discharge estimates. Discharge estimates for the two events were scaled proportionally across this roughness range, and the flow–area regressions were recomputed to evaluate the sensitivity of the fitted exponent.

3. Results

3.1. Operational period

Operational periods for the 136 stations ranged from 0.6 to 113.0 years (Fig. 4a). The mean and median operational period of WMIP stations were 26.8 and 20.2 years, respectively. Gauge 130302A (Dawson River at Taroom) has by far the longest data record, with the station operational since 1911. Station 130305A (Dawson River at Theodore) has the second-longest operational period (78.4 years) but the site was closed in July 2002.

Most gauging stations operational for over 45 years are still active now (Fig. 4b). Conversely, a majority of sites with shorter activity periods have been decommissioned. In several instances, a gauge was relocated or replaced, reflected by the lettering system of the site ID. For example, 130003A and 130003B (Fitzroy River at Riverslea) have been operational for 49.3 and 52.5 years, respectively, with 130003A replaced by 130003B in October 1974.

Peak coverage was from 3 June 1987 to 28 February 1988, with 79 gauges operational within the Fitzroy Basin (Fig. 4b). Since early July 2002, the number of active stations has stabilised at around 45.

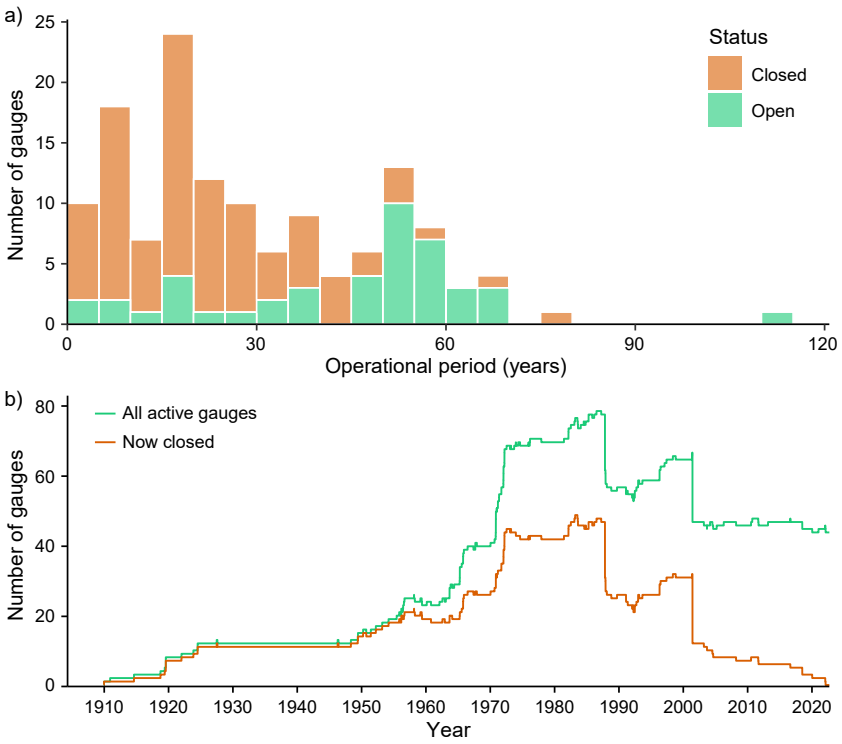

Fig. 4. a) Distribution of Fitzroy Basin stream gauges by operational period as of 1 January 2024 (bin width: 5 years). b) Timeseries of the daily number of active gauges and those still operational in early 2024.

3.2. Catchment area vs specific discharge

Specific discharge (discharge per unit catchment area) is inversely related to catchment size, but the relationship is highly nonlinear (Fig. S1). Consequently, both the area and specific discharge were logarithmically transformed (Fig. 5). The application of flow–area scaling highlights scale-invariant behaviour in peak streamflow across the Fitzroy Basin.

Fig. 5a illustrates that most nested catchments within the Fitzroy Basin have comparable trends, despite variable operational periods and peak discharge events (Fig. 5b). The Isaac River subcatchment is the only subset without an inverse relationship between A_{log} and q_{log} (Fig. 6d; $r = 0.04$, $p = 0.947$, $n = 6$). Although this may suggest that specific discharge is governed by factors other than upstream area, this upper subcatchment also has a relatively small log-linear range, with far-upstream sites not monitored (smallest area: 344 km^2; Table 3). Except for the Connors ($r = -0.54$, $p = 0.083$, $n = 11$; Fig. 6b) and Don ($r = -0.38$, $p = 0.105$, $n = 19$; Fig. 6f) river systems, all inverse relationships are statistically significant at $\alpha = 0.05$ (Table 3). Gauges from the Connors River subcatchment stand out by relatively elevated q_{log}, aligning with the wetter conditions of that region (Fig. 2a).

A sensitivity analysis of peak-flow estimates and operational record length is presented in Section 3.3.

3.3. Sensitivity analyses

The two most extreme peak discharge estimates derived from WMIP (130401A in 2017 and 130003A in 1954) were recalculated using a range of Manning's n_M to assess the sensitivity of the flow–area relationship to hydraulic assumptions. For both gauging stations, peak discharge was recomputed by assuming a WMIP-applied n_M of 0.06 and a plausible range of 0.035–0.090, equating to a maximum flow rate decrease of 33% or an increase of up to 71%. These bounds correspond to uncertainty ranges of 15,893–40,867 m^3/s for 130401A and 13,035–33,519 m^3/s for 130003A.

Despite these site-level differences, the basin-wide regression between q_{log} and A_{log} was stable, with the exponent γ remaining −0.55 across the tested n_M range (Fig. S2a,b). Subcatchment-specific exponents showed similarly limited sensitivity for the Fitzroy River and Connors River subcatchments, with γ changing by only 0.01 (−0.68 to −0.67; Fig. S2g,h) and 0.11 (−0.50 to −0.39; Fig. S2c,d), respectively. The Isaac River subcatchment exhibited the greatest variation, ranging from −0.08 to +0.12 (Fig. S2e,f).

Fig. 7 highlights the influence of short-record stations on the strength of the flow–area relationship. Removing gauges 130359A and 130337A produces a marked improvement in both *r*- and *p*-values. As additional short-record sites are excluded, the correlation generally strengthens until an operational period of approximately 22.5 years ($r = -0.865$, $p < 10^{-22}$, $n = 71$) is reached. The relationship then plateaus until sites with operational periods shorter than about 52 years are excluded, with the CI gradually widening as sample size declines. From around $n = 25$, the correlation becomes increasingly unstable, with reduced statistical confidence as sample size declines. The *p*-value exceeds 0.001 at $n = 11$ ($r = -0.822$).

These results show that both hydraulic assumptions and record length affect individual peak-discharge estimates. However, neither materially altered the overall inverse scaling between catchment area and peak specific discharge.

4. Discussion

4.1. Flow–area scaling law

The power-law scaling of peak specific discharge in the Fitzroy Basin is broadly consistent with previously reported β values for large, heterogeneous basins, although direct comparisons are limited by differences in study design and data type. The exponent γ of individual major subcatchments varies from −0.67 in the Fitzroy River to 0.01 in the Isaac River (corresponding to $\beta = 0.33$–1.01), with a basin-wide value of −0.55 ($\beta = 0.45$; Fig. 6a,d,j). The results are based on peak historical

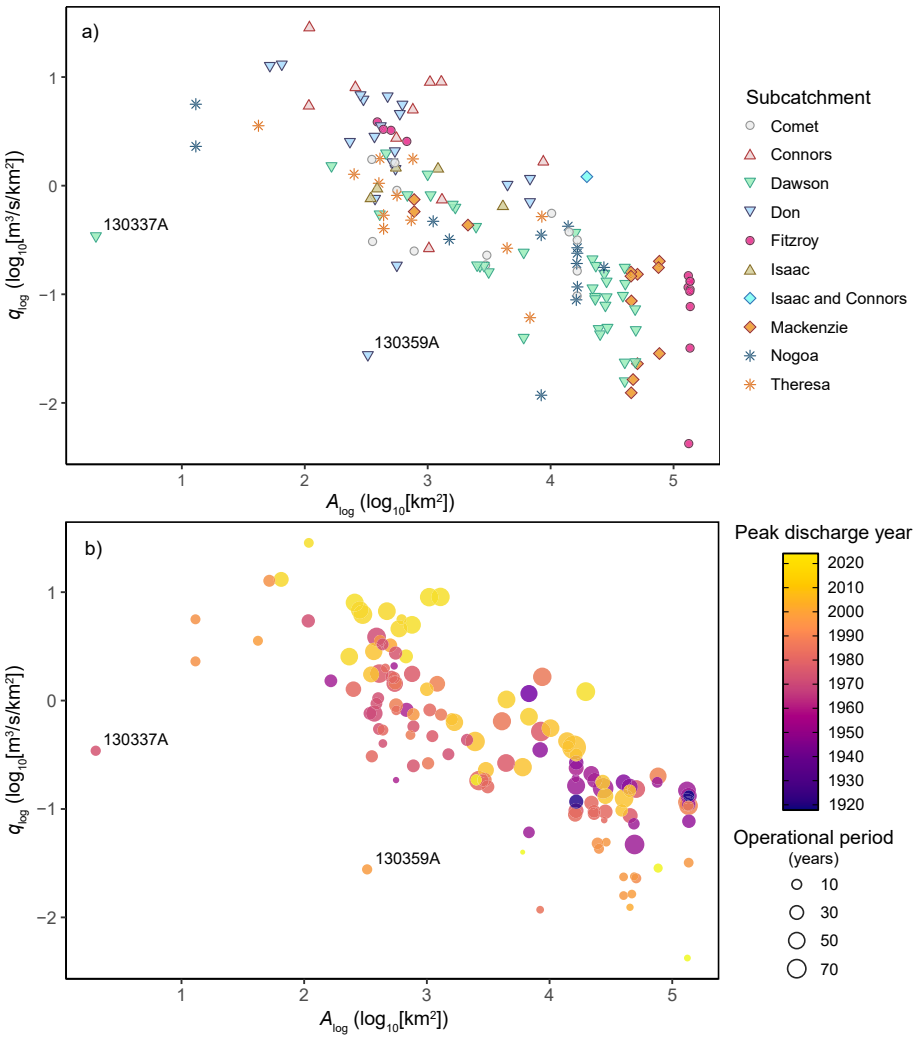

Fig. 5. Log–log relationship between catchment area (A_{log}) and peak specific discharge (q_{log}) within the Fitzroy Basin. Panel a) shows subcatchment identifiers. Panel b) uses symbol size to represent operational period and colour to indicate the year of peak discharge.

flows at individual gauging sites. Ghanbarian (2025) highlighted that β tends to be larger for smaller catchments, a tendency also evident in the Fitzroy Basin subcatchments (Table 3).

Several subcatchment regressions are statistically non-significant, which is attributed to three main factors: 1) absence of monitoring at far upstream sites, 2) stronger hydrological affiliation of peak streamflow with adjacent subcatchments and 3) short operational periods. For example, lower-order creeks in the Isaac River subcatchment tend to be dry throughout most of the year. Such non-perennial sites are rarely monitored, as illustrated by the gauge with the smallest area (344 km^2; Table S2) within that subcatchment. The inclusion of lower-order ephemeral streams in the Isaac River peak-flow analysis would likely have steepened the log-linear slope (γ), because upstream sites in the Cwa climate zone (Fig. 1) are expected to exhibit distinctly higher specific discharge despite only flowing briefly. Furthermore, the most downstream gauge on the Isaac River (130401A) tends to more closely represent extreme flows of the Connors River because of that catchment's typically much greater rainfall (Fig. 2; Table 2). Unlike the Isaac River, the non-significant results for the Connors and Don rivers are ascribed to sites operational for a relatively brief period and their consequently lowered opportunity to capture an extreme flow event, as further discussed in Section 4.1.1.

Most published studies report β for average conditions over a defined period (e.g. annual) or event-based peak discharges rather than site-specific historical peaks, as in the present analysis. For example, Smith (1992) reported β values of 0.65–0.69 for mean annual flood peaks in central Appalachian basins (0.78–26,100 km^2), comparable to the Comet River (β = 0.66; 351–16,457 km^2; Fig. 6g and Table 3). Conversely, Chen et al. (2019) calculated a median β of 0.82 for 52 peak-discharge events in the Iowa River Basin over 12 years, using the dataset compiled by Ayalew et al. (2015). This translates to γ = –0.18 when expressed in terms of specific discharge, reflecting a weaker dependence on catchment area compared with the Fitzroy Basin. The Iowa River Basin (33,000 km^2) is substantially smaller than the Fitzroy Basin (143,000 km^2) and Ayalew et al. (2015) selected rainfall–runoff events exhibiting basin-wide coverage, with both factors reducing spatial variability. Consequently, although the positive relationship between discharge and catchment area tends to be stronger in smaller catchments (i.e. larger β), the generally inverse connection between specific discharge and area is weakened (γ closer to zero).

In addition to catchment size and event selection, differences in exponent magnitude between studies can also be attributed to operational period, rainfall characteristics, and basin attributes like drainage network geometry and topography (e.g. Ayalew et al., 2015). The Fitzroy Basin is substantially larger (143,000 km^2) and more hydrologically heterogeneous than most basins previously studied, likely contributing to the wider range of observed scaling exponents. Additionally, influential stations and differences in operational period affect slope estimates, as highlighted in Fig. 7, underscoring the sensitivity of γ to both data coverage and extreme events. Two gauges in particular, 130359A

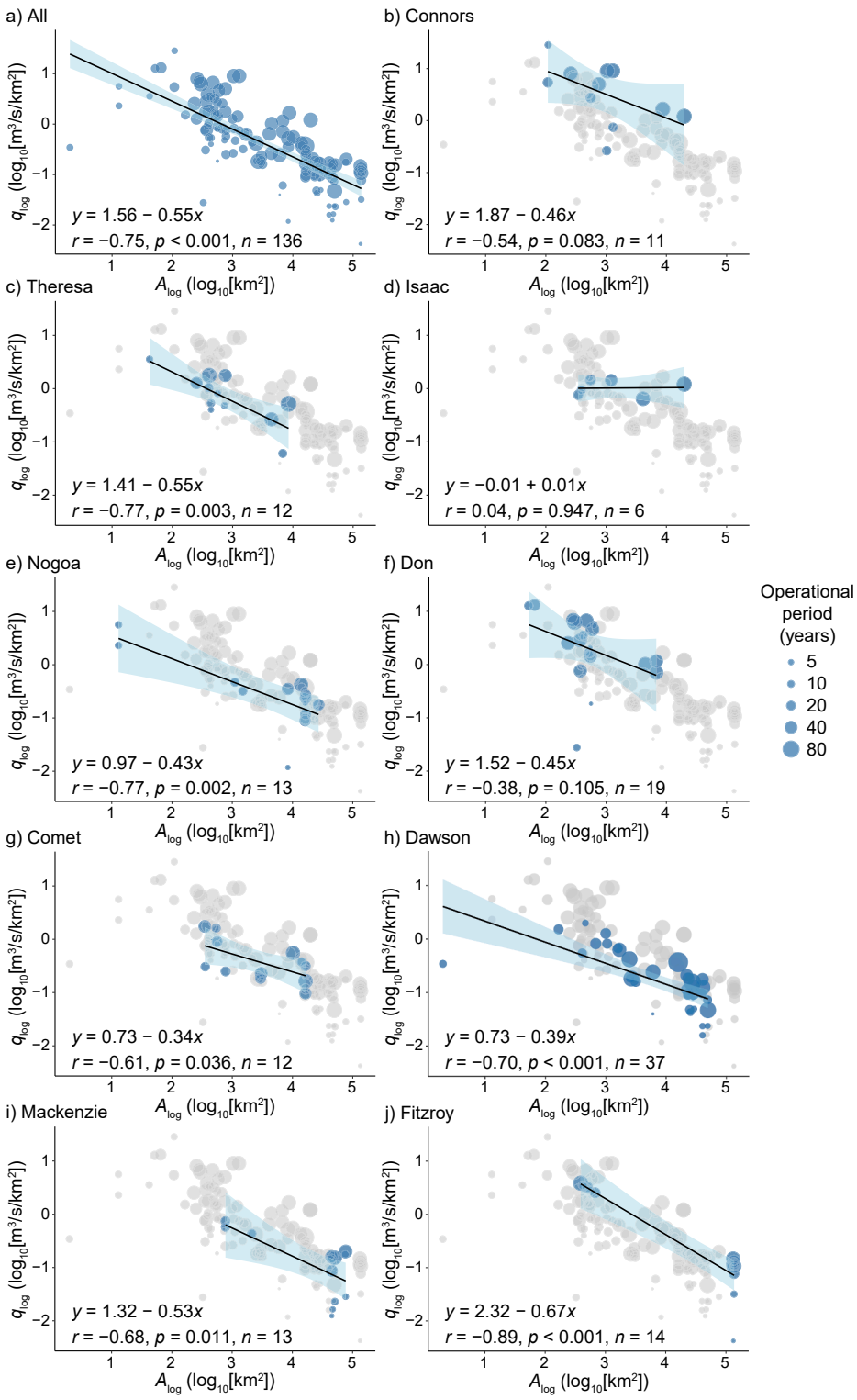

Fig. 6. Regression between log-transformed catchment area (A_{log}) and specific discharge (q_{log}) for a) all sites and the subcatchments of b) the Connors River, c) Theresa Creek, d) the Isaac River, e) the Nogoa River, f) the Don River, g) the Comet River, h) the Dawson River, i) the Mackenzie River, and j) the Fitzroy River. The shaded band represents the 95% confidence interval of the fitted regression line. Gauge 130401A (Isaac River at Yatton) is included in both b) and d). Blue markers indicate gauging stations included in the regression, and grey markers show excluded data.

and 130337A, exert disproportionate influence on the scaling relationships because of their short operational periods and – in the case of 130337A – atypical catchment area. Section 4.1.1 examines how operational period and catchment area affect the stability of the observed A_{log}–q_{log} scaling relationships.

4.1.1. *Operational period and catchment area*

Streamflow recordings are not always continuous, and data gaps spanning several months or years can therefore overstate the operational period. Gauging stations may also be damaged by extreme flow events, resulting in data gaps and the possible exclusion of streamflow peaks.

Table 3
Summary of subcatchment-specific regression results between log-transformed catchment area (A_{log}) and specific discharge (q_{log}; Fig. 6). For each region, the number of included sites, the range of upstream catchment area and operational period, and the regression parameters (r, p and γ) are listed, along with the corresponding total-discharge exponent (β) derived from γ. Site-specific details are provided in Table S2.

Subcatchment	Site count (n)	Specific-discharge regression			Total-discharge exponent β	Catchment area (km^2)	Operational period (years)
		r	p	γ			
All	136	−0.75	<0.001	−0.55	0.45	2–136,635	0.6–113.0
Comet	12	−0.61	0.036	−0.34	0.66	351–16,457	15.9–54.3
Connors	11	−0.54	0.083	−0.46	0.54	108–19,719	8.0–61.3
Dawson	37	−0.70	<0.001	−0.39	0.61	2–49,293	0.6–113.0
Don	19	−0.38	0.105	−0.45	0.55	52–6,795	1.2–63.2
Fitzroy	14	−0.89	<0.001	−0.67	0.33	389–136,635	1.7–60.3
Isaac	6	0.04	0.947	0.01	1.01	344–19,719	15.4–61.3
Mackenzie	13	−0.68	0.011	−0.53	0.47	776–76,715	2.3–52.4
Nogoa	13	−0.77	0.002	−0.43	0.57	13–27,130	3.0–51.9
Theresa	12	−0.77	0.003	−0.55	0.45	42–8,485	5.0–68.0

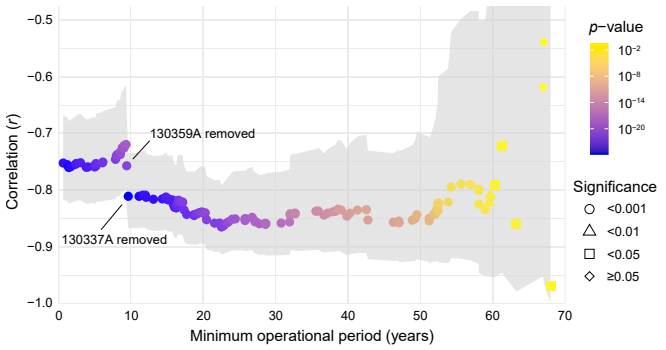

Fig. 7. Correlation (r) between log-transformed catchment area (A_{log}) and specific discharge (q_{log}) as a function of the minimum operational period of included gauging stations. The colour scheme represents the p-value and the symbol reflects the significance category. The grey band indicates the 95% confidence interval based on the Fisher z-transformation.

The longer a stream gauge is active, the higher its probability of capturing a record flow event. However, even a site operational for a very short period can register such an event triggered by stochastic, chaotic weather systems. For example, 130001A was operational for only 13.1 years but recorded the Great Flood of 1918, the most severe recorded flood event on the Fitzroy River.

Runoff variability is particularly evident in the presence of outliers in the flow–area relationship, which tend to be associated with stream gauges operational for less than a decade. In most instances, the more extreme outliers are points below the trendline (Fig. 6), indicating lower specific discharge than expected for the catchment size. Two data points are distinctly below the main cluster (Fig. 5b): 130359A (Kroombit Creek at Kroombit Dam Tailwater) and 130337A (DPI Moura Gully at Crump Weir), with operational periods of 9.3 and 9.4 years, respectively. Given the rarity of extreme rainfall–runoff events, short operational periods reduce the likelihood of capturing rare, high-magnitude events, potentially biasing scaling relationships.

Another distinguishing feature of 130337A is its unusually small catchment size (2 km^2), with 130220A (LN1 Drain at Emerald) and 130221A (LN3 Drain at Selma Road) having the next-lowest areas (13 km^2; Table S2). 130359A is the only site for which the catchment area (326 km^2) was obtained directly from the WMIP website, with the downloaded site description not including this information. The catchment area (373 km^2) at nearby 130321A (Kroombit Creek at Mt. Kroombit), located further downstream, suggests that the 130359A estimate is reasonable. Consequently, its outlier status is more related to its short operational period than to an inexact upstream area estimate.

Excluding the short-record outliers 130359A and 130337A substantially improves the strength and stability of the scaling relationship between area and specific-discharge yields (Fig. S3) compared with Fig. 7, particularly in the subcatchments of the Don and Dawson rivers, highlighting their outsized influence. Gauge 130359A also weakens the regression for the Don River subcatchment (Fig. 6f). Its removal ($n = 18$) reduces the p-value to 0.006 and improves the r-value to −0.62 (Fig. S4a). The relationship for the Dawson River system is similarly enhanced by omitting 130337A ($r = -0.83$, $p < 0.001$, $n = 36$; Fig. S4b), because its extremely low catchment area exerts a disproportionately large effect on the regression slope.

When the Connors River subcatchment is viewed in isolation (Fig. 6b), two gauges (130411A and 130412A) are distinctly below the linear regression of the log–log graph, with both having relatively short operational periods (16.8–17.3 years). However, unlike 130359A and 130337A, the two gauges are well aligned with peak historical specific discharge for the Fitzroy Basin (Fig. 5a).

Some minor discrepancies in catchment area were noted for some sites, although these would have a negligible effect on the specific-discharge estimate. One such discrepancy includes 130001B (Fitzroy River at Mc Murdos; 136,635 km^2). Despite its position slightly upstream from 130001A and 130001C (Fitzroy River at Yaamba; 136,398 km^2), the gauge is attributed a slightly larger catchment area (+237 km^2) than its two downstream counterparts.

The iterative record-length analysis (Fig. 7 and Fig. S3) evaluates basin-scale temporal sampling effects by progressively removing gauges with short operational histories. This approach isolates the influence of record length on the stability of the fitted exponent γ. However, subcatchment-specific variability in γ reflects additional factors, particularly spatial heterogeneity in geomorphological setting and climatic regime. The 22.5-year operational-period threshold therefore represents a basin-scale stability property rather than a diagnostic tool for explaining subcatchment-level variability.

Basins containing subcatchments with strong contrasts between hillslopes, confined channels and floodplain reaches are expected to exhibit a wider range of γ values because of these underlying hydro-geomorphological differences. In the Fitzroy Basin, the Isaac River subcatchment is dominated by ephemeral upland channels, the Connors River subcatchment includes steep upper reaches, and the lower Mackenzie River contains anabranching sections. The main Fitzroy River, by contrast, alternates between broad lowland floodplains with extensive overbank inundation and narrow, confined passages (e.g. upstream from 130005A). These contrasting geomorphological domains influence flood-wave propagation, attenuation and peak-discharge behaviour, contributing to the divergence in γ values. Recent work by Costabile et al. (2024) has shown that spatial heterogeneity in inundation patterns and transitions between geomorphological units can strongly affect flood dynamics, supporting the interpretation that geomorphology plays a role alongside operational record length and rainfall extent.

4.2. Controls of hydroclimate and rainfall extent on peak discharge

Hydroclimatic drivers influence both the magnitude and spatial coherence of peak flows and therefore shape the observed scaling behaviour, particularly in large basins where rainfall patterns vary markedly in space and time. Rainfall events are more likely to encompass smaller catchments entirely, producing higher specific discharge, whereas larger catchments (e.g. the entire Fitzroy Basin) are less likely to be uniformly affected. Even when rainfall spans nearly the entire basin, tributary inputs are likely asynchronous because of catchment scale, spatial heterogeneity and network complexity (Fig. 1; e.g. Blöschl and Sivapalan, 1995), reducing the combined downstream peak.

Large-scale precipitation events encompassing the entire Fitzroy Basin are uncommon, and extreme flow events throughout the basin are similarly rare. However, intense rainfall in upstream catchments can produce extensive flooding downstream, even where local rainfall has been limited. Diverse weather systems can generate elevated flows of varying duration and magnitude, including intense scattered showers from inland storms, frontal systems and atmospheric lows such as TCs and remnant lows (Higgins et al., 2022; Jaffrés et al., 2022). Within the Fitzroy Basin, extreme streamflow events are commonly associated with TCs, tropical lows or monsoon lows. Well-positioned TCs can have basin-wide impacts on streamflow, whereas thunderstorms tend to be brief and spatially confined.

One of the most widespread rainfall–runoff events occurred during the prolonged 2010/2011 Queensland floods under a very strong La Niña. The southern oscillation index (SOI) remained exceptionally high throughout most of the 2010/2011 austral summer, with monthly values in December and February–April ranking among the highest on record based on data from the Australian Bureau of Meteorology (1876–2024; https://www.bom.gov.au/climate/enso/soi/). Several TCs crossed the northeastern Queensland coast during this period, bringing extensive rainfall to an already saturated region. With each successive rainfall event, rivers responded with increasing intensity, reflecting cumulative catchment saturation. Between 23 December and 2 January, 18 gauges reached record peaks (Fig. 8a). Several of these coincided with the passage of TC Tasha over Christmas 2010. The affected area was widespread, with new discharge records reached in the Comet, Dawson, Don, Mackenzie and Nogoa River subcatchments.

However, elevated streamflow is not confined to periods when remote teleconnections are favourable or to the height of the wet season. The 1982/1983 water year coincided with a very strong El Niño, reflected in both the SOI and sea surface temperature. Despite generally very dry conditions throughout the year, 13 stations reached record levels between 1 and 8 May, with a fourteenth doing so later in the month (Fig. 8a). The spatial extent was more limited, however, with only three subcatchments affected: Theresa Creek, and the Comet and Dawson rivers.

Another El Niño water year is credited with the largest recorded discharge in the Fitzroy River, measured at 130003A (Fitzroy River at Riverslea), with an estimated 19,553 m^3/s on 15 February 1954. The gauge's catchment area is 131,883 km^2, representing approximately 92.2% of the total basin area. Runoff from most of the Fitzroy Basin would therefore have passed through this site. Actual peak discharge into Keppel Bay may have exceeded this value, depending on rainfall and flow attenuation processes in the lower basin, which accounts for

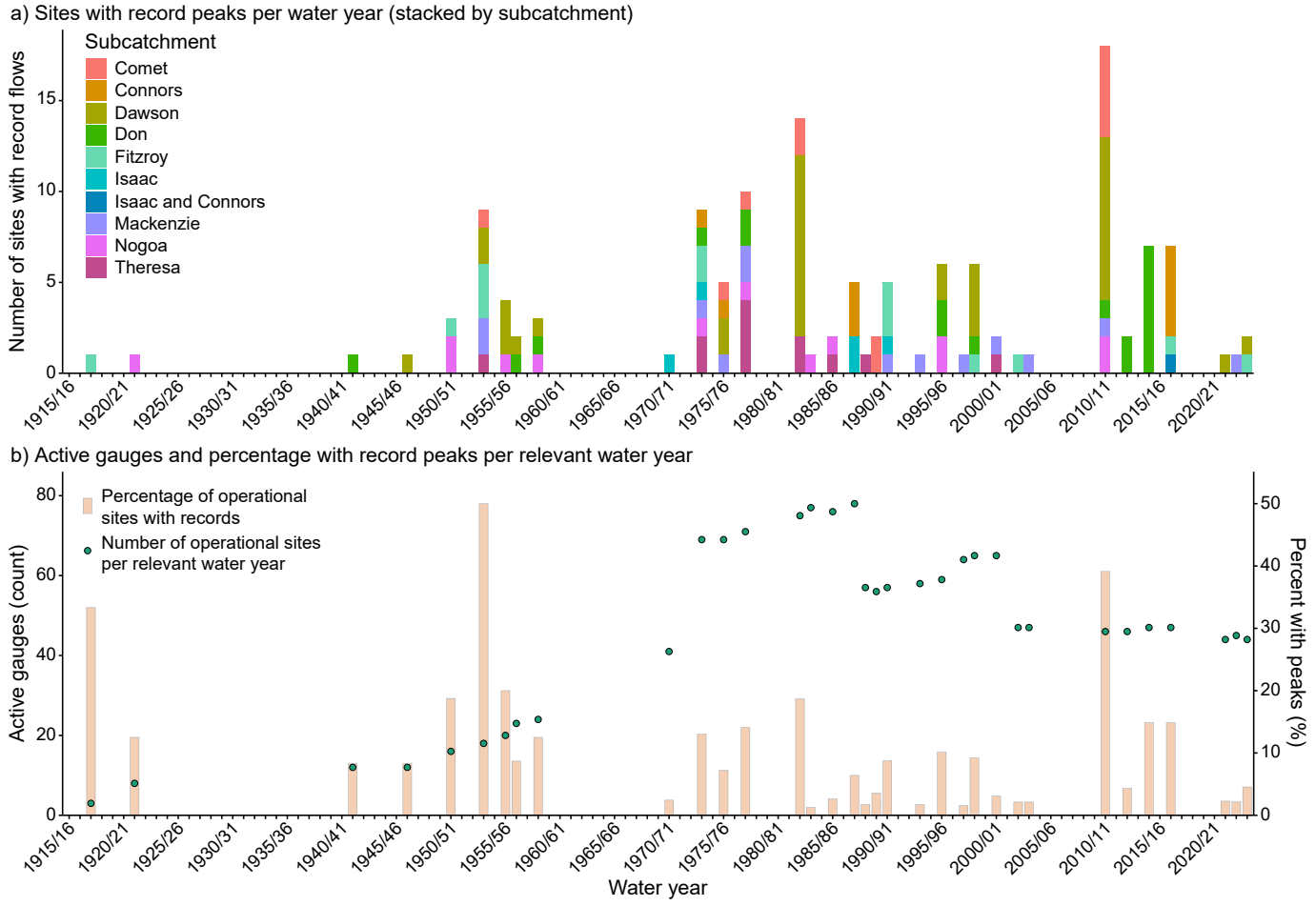

Fig. 8. a) Number of sites with record flows per water year and subcatchment. b) Number of active gauges during the relevant months of each water year that have flow records, and the percentage of these gauges that registered a peak flow. The water year is defined as September to August.

about 7.8% of the total area downstream from 130003A. Besides the lower Fitzroy Basin, discharge records were also obtained for four other subcatchments (Comet, Dawson and Mackenzie rivers, and Theresa Creek). Notably, half of the gauges operating at the time (9 out of 18) registered record flow rates (Fig. 8b). This flood event is associated with a tropical low that crossed the coast north of the basin on 7 February 1954 and moved southwestward overland, passing west of the Fitzroy Basin and bringing widespread rainfall to the catchment.

The effect of flow attenuation processes – the reduction or dampening of the magnitude of a hydrograph peak – is evident in the record flow event produced by severe TC Debbie in late March 2017. The TC moved through the basin from north to south during its passage, in the same direction as the major streams, thus exacerbating flooding in downstream areas. Previous studies (e.g. de Lima and Singh, 2002) have demonstrated that flood peaks tend to be greater for storms moving downstream within a catchment. Hence, the pathway of TC Debbie intensified rainfall impacts on river levels in the lower Fitzroy Basin. It produced the highest recorded flow (23,839 m^3/s on 30 March 2017), attributed to 130401A (Isaac River at Yatton), situated after the confluence with the Connors River. The subcatchment area (19,719 km^2; Table S2) covers about 13.8% of the basin and its northeastern Connors Range is often associated with the most intense rainfall. By the time the floodwaters from the northeast reached the Fitzroy River, flow attenuation reduced flow volumes to 11,806 m^3/s (130003B, Fitzroy River at Riverslea on 3 April 2017). Overall, 7 of 47 operational gauges registered record flows, mostly in the Connors River subcatchment. The single record in the Fitzroy River subcatchment is associated with a small, southward-flowing tributary to the Fitzroy River (Marlborough Creek).

The third-highest discharge in the basin is attributed to 130001A (Fitzroy River at Yaamba) on 31 January 1918, during the Great Flood. This rainfall event was associated with a severe TC that crossed the coast just north of Mackay (Callaghan and Power, 2011). Only three sites were operational at the time, with the two other gauges monitoring the Dawson River. Consequently, no gauge data are available for most of the basin.

The 1973/1974 water year saw the largest number of nested catchments registering peak discharge, with nine gauges located across seven subcatchments (Fig. 8a). All subcatchments except those of the Dawson and Comet rivers recorded new peaks. This was another year of a relatively strong La Niña, which brought wet conditions across much of Australia. Several flow records coincided with TCs, including TC Una in mid-December 1973. Offshore TCs Vera and Wanda also contributed to sustained soil saturation and high catchment responsiveness, particularly in the eastern subcatchments during mid-February.

These hydroclimatic patterns help explain why some subcatchments deviate from the basin-wide scaling exponent. However, the ability of stream gauges to accurately record extreme flows is also constrained by rating-curve limitations and the complexity of channel cross-sections, independent of the hydroclimatic drivers discussed above. Section 4.3 examines how these measurement uncertainties influence the interpretation of peak discharge records.

4.3. Stream gauge capacity to record extreme flow: rating curves and flood damage

Potentially large errors in rating curves – the conversion from river height to discharge – arise from complex or non-stationary channel profiles, making accurate runoff estimates challenging. Reliable runoff analysis based on observational data therefore depends heavily on accurate conversion of measured river heights to corresponding discharge volumes.

Major creeks in the Fitzroy Basin typically feature deep channels with distinct low-flow, medium-flow and high-flow banks. This configuration is generally present on both sides of the channel, although it may be asymmetric. Beyond the high-flow banks lie extensive floodplains. During extreme flow conditions, as little as 10% of floodwater may remain within streambanks, whereas the remaining 90% spreads across the floodplains.

Gauging stations are generally positioned to record primarily in-bank flows and typically do not capture the full extent of out-of-bank flows, which can sometimes exceed 80–90% of total discharge during large floods. Consequently, rating curves are applicable mainly to in-bank conditions, necessitating empirical estimates for additional flow across the floodplain. These estimates often rely on indicators such as flood lines on trees and debris on fence posts. Flow velocity across the floodplain is estimated from gradients and adjusted for the effects of vegetation and surface roughness using the Manning's roughness coefficient.

Many stream gauges are unable to provide accurate discharge estimates during extreme flow events. In some cases, a portion of the flow may bypass or be diverted around the gauge. Furthermore, channel cross-sections are not always stationary and can be highly complex. In the Fitzroy Basin, for example, floodplains can extend over several kilometres. This is illustrated by station 130401A (Isaac River at Yatton), where the flood height of 19.675 m during TC Debbie inundated a width of nearly 5 km (Fig. 9). Beyond about 15.7 m – the height of the main channel at 130401A – uncertainty in converting water level to discharge increases progressively. Other gauges in the basin have even wider floodplain profiles.

Estimation of reasonable Manning's n_M values for broad, out-of-bank flow is challenging in the seasonally arid tropics. Although Arcement and Schneider (1989) provide guidance, their principles are difficult to apply in detail. The two sites (130401A and 130003A) that recorded the largest discharges are described by WMIP as *sand gravel* and *rock outcrop*, respectively. These descriptions relate to the stream bed rather than the wider floodplain. Sand and gravel indicate a mobile bed with moderate roughness, typically $n_M = 0.025–0.035$ for the channel. Rock outcrops reflect immobile beds with slightly lower roughness (approximately $n_M = 0.020–0.030$ for the channel). In contrast, floodplain roughness is much higher because of surface vegetation (grass, shrubs, trees), fences and uneven ground. Because WMIP's channel descriptions imply roughness values of approximately $n_M = 0.020–0.035$, the adopted range of $n_M = 0.035–0.090$ spans from the upper end of typical channel roughness to plausible vegetated floodplain conditions during extreme inundation.

Manning's n_M also varies seasonally with vegetation density and within individual events because of soil saturation and progressive flattening of ground cover by rising flows, which increases conveyance. At the end of the dry season, vegetation cover is sparse and many of the soils develop a surface crust. During the wet season, vegetation may be prolific and surface crusts are absent. Late wet-season conditions – when riparian and floodplain vegetation is most abundant – yield higher roughness values than the same cross-section during the dry season or late in a major flood. The range adopted here is intended to bracket these conditions.

Additional complexity arises from the pulsed nature of extreme rainfall in the seasonally arid tropics: early precipitation cells tend to flatten low vegetation such as grasses, reducing resistance to subsequent flow pulses. Floodplain heterogeneity – including agricultural land use, irrigation status, and variable soil and vegetation types across broad, unchannelled areas – further complicates coefficient estimation. Considering these factors alongside direct observation, a range of $n_M = 0.035–0.090$ with a central value of 0.06 is considered reasonable.

Rating-curve uncertainty increases at extreme stages where floodplain inundation exceeds the calibrated range. For the two largest events (130401A in 2017 and 130003A in 1954), plausible Manning's n_M for vegetated floodplains (0.035–0.090; Arcement and Schneider, 1989) imply an uncertainty range of approximately −33% to +71% when $n_M = 0.06$ is assumed for the original WMIP estimate. A simple sensitivity test in which these upper-tail discharges were varied within these bounds showed that the basin-wide scaling relationship remained

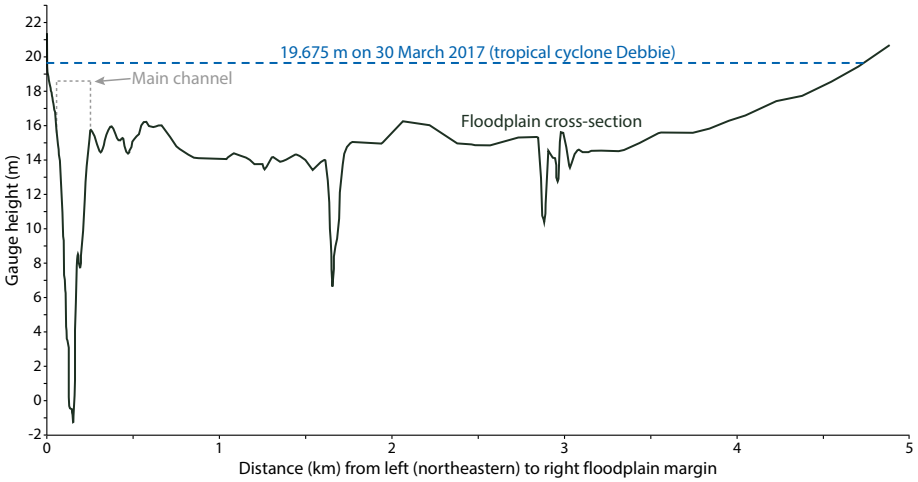

Fig. 9. Cross-section at station 130401A (Isaac River at Yatton), redrawn from the latest image on the Water Monitoring Information Portal (accessed on 18 October 2025), showing the full floodplain. The peak historical river height is indicated across the floodplain, and the main channel is marked in grey. Vertical exaggeration is approximately 1:100 (10 m per km).

significant, with the fitted exponent γ stable at −0.55. This indicates that the basin-scale peak-area relationship is robust to plausible uncertainty in the largest discharge estimates.

The Isaac River subcatchment showed the greatest variation in γ across the tested roughness range. This reflects both its small sample size ($n = 6$) and the influence of gauge 130401A, which primarily captures extreme flows originating in the Connors River system rather than the Isaac River headwaters. The original Isaac River regression was near-horizontal and statistically non-significant, and although γ varied from −0.08 to +0.12 under the sensitivity scenarios, it remained non-significant throughout. This behaviour is therefore attributable to sampling limitations rather than sensitivity of the underlying scaling. The results for the Connors River were similarly non-significant across all scenarios.

4.4. Non-stationary climate

Projected increases in atmospheric moisture with warming climate are expected to intensify rainfall events, particularly short-duration, high-intensity storms (Li et al., 2019; Visser et al., 2023; Wasko et al., 2024). This shift may steepen hydrograph peaks during extreme events (Wasko et al., 2021), as catchments respond more rapidly to concentrated precipitation inputs. Extreme rainfall intensities have already increased in many regions, including parts of Australia, with subhourly rainfall intensities near Sydney rising by at least 20% per decade from 1999 to 2017 (Ayat et al., 2022). Such changes reduce the effectiveness of natural (e.g. antecedent soil moisture) and engineered flow attenuation, potentially overwhelming detention basins, wetlands and channel storage. The magnitude and frequency of flood peaks are projected to rise in many catchments, driven by both thermodynamic and convective enhancements in precipitation. Sharma et al. (2018) specifically highlighted that the rarest floods are more likely to increase at higher temperatures, especially in smaller catchments. In the Fitzroy Basin, such trends underscore the need to reassess design thresholds and flood mitigation strategies, particularly in rapidly responding catchments where steepened peaks may exacerbate downstream flood risks.

5. Conclusions

Peak specific discharge in the Fitzroy Basin follows a strong inverse power-law relationship with catchment area. However, the magnitude and stability of the scaling exponent vary systematically with operational record length, rainfall extent and subcatchment characteristics. Using site-specific historical peak flows across a large, hydrologically diverse basin, this study provides a comprehensive assessment of extreme-flow scaling with catchment area. The analysis demonstrates that gauges with longer operational records are more likely to capture rare, high-magnitude flow events. In contrast, gauges with short operational periods disproportionately weaken scaling relationships, with specific stations identified whose influence on the scaling exponent is substantial. Log-linear scaling parameters for the subcatchments align well with previous studies, with larger subcatchments tending to have lower exponents because of greater rainfall–runoff variability. These findings offer practical guidance for selecting gauges in future scaling analyses and flood-frequency assessments.

The fitted exponents for the major subcatchments provide parameters that can inform regional hydrological modelling and design applications, particularly where nested catchments require consistent representation of extreme flows. Projected increases in rainfall intensity may steepen scaling in upper catchments, whereas downstream attenuation may moderate these effects, influencing the slope of the log–log scaling relationship. This has implications for forecasting frameworks that rely on spatial scaling of peak discharge.

Uncertainties in rating curves and non-stationary channel cross-sections remain key limitations when estimating extreme flows, particularly in complex, wide floodplains extending over several kilometres. Nevertheless, varying the two largest discharge estimates across a plausible range of Manning's roughness coefficients ($n_M = 0.035–0.090$) showed that the basin-wide scaling relationship remained robust, with γ stable at −0.55. Improved empirical characterisation of out-of-bank flows and revised design thresholds in flood-prone catchments would enhance the reliability of peak-flow scaling in large basins.

Despite these challenges, this study provides parameters and insights that support management decisions, hydrological forecasting, model calibration and flood-risk assessment, offering a framework to predict extreme streamflow responses across nested catchments under current and future climatic conditions.

CRediT authorship contribution statement

Jasmine B.D. Jaffrés: Writing – review & editing, Writing – original draft, Visualization, Validation, Software, Methodology, Investigation, Formal analysis, Data curation, Conceptualization. **Chris Cuff:** Writing – review & editing, Investigation, Funding acquisition, Conceptualization. **Cecily E. Rasmussen:** Investigation, Funding acquisition, Conceptualization.

Declaration of competing interest

The authors declare that they have no known competing financial interests or personal relationships that could have appeared to influence the work reported in this paper.

Acknowledgements

The authors wish to acknowledge the late Mr Geoff Cavanagh, whose insights and discussions inspired many of the ideas developed in this paper. Although Geoff had no formal qualifications, he was among the finest surface hydrologists C. Cuff and C. E. Rasmussen have known, drawing on extensive experience as an irrigation farmer in the Fitzroy Basin, within the seasonally arid tropics.

This paper draws on work conducted for an unpublished report finalised in 2025 by the same author team for Suncorp Insurance, which commissioned and funded the study. The manuscript was fully rewritten for journal publication, incorporating new analyses and methods.

Rainfall data were extracted from the SILO database (https://www.longpaddock.qld.gov.au/silo/point-data) for the period of 1950 to 2025. The southern oscillation index (SOI) data were accessed from the Australian Bureau of Meteorology (1876–2024; https://www.bom.gov.au/climate/enso/soi/).

Appendix A. Supplementary data

Supplementary data to this article can be found online at https://doi.org/10.1016/j.jhydrol.2026.135535.

Data availability

Data will be made available on request.

References

Arcement, G.J., Schneider, V.R., 1989. Guide for selecting Manning's roughness coefficients for natural channels and flood plains. US Geological Survey 44, pp.
Ayalew, T.B., Krajewski, W.F., Mantilla, R., 2015. Analyzing the effects of excess rainfall properties on the scaling structure of peak discharges: insights from a mesoscale river basin. Water Resour. Res. 51 (6), 3900–3921.
Ayat, H., Evans, J.P., Sherwood, S.C., Soderholm, J., 2022. Intensification of subhourly heavy rainfall. Science 378 (6620), 655–659.
Beck, H.E., Zimmermann, N.E., McVicar, T.R., Vergopolan, N., Berg, A., Wood, E.F., 2018. Present and future Köppen-Geiger climate classification maps at 1-km resolution. Sci. Data 5, 180214.
Blöschl, G., Sivapalan, M., 1995. Scale issues in hydrological modelling: a review. Hydrol. Process. 9 (3–4), 251–290.
Callaghan, J., Power, S.B., 2011. Variability and decline in the number of severe tropical cyclones making land-fall over eastern Australia since the late nineteenth century. Clim. Dyn. 37 (3), 647–662.
Castellarin, A., Vogel, R.M., Brath, A., 2004. A stochastic index flow model of flow duration curves. Water Resour. Res. 40 (3).
Chen, B., Ma, C., Krajewski, W.F., Wang, P., Ren, F., 2019. Logarithmic transformation and peak-discharge power-law analysis. Hydrol. Res. 51 (1), 65–76.
Costabile, P., Costanzo, C., Lombardo, M., Shavers, E., Stanislawski, L.V., 2024. Unravelling spatial heterogeneity of inundation pattern domains for 2D analysis of fluvial landscapes and drainage networks. J. Hydrol. 632, 130728.
de Lima, J.L.M.P., Singh, V.P., 2002. The influence of the pattern of moving rainstorms on overland flow. Adv. Water Resour. 25 (7), 817–828.
Galster, J.C., 2007. Natural and anthropogenic influences on the scaling of discharge with drainage area for multiple watersheds. Geosphere 3 (4), 260–271.
Ghanbarian, B., 2025. Non-linearity in mean annual peak flow scaling with upstream basin area: insights from percolation theory. Ecohydrology 18 (2), e2709.
Gupta, V.K., Waymire, E.C., 1998. Spatial variability and scale invariance in hydrologic regionalization. In: Sposito, G. (Ed.), Scale Dependence and Scale Invariance in Hydrology. Cambridge University Press, Cambridge, pp. 88–135.
Higgins, P.A., Palmer, J.G., Rao, M.P., Andersen, M.S., Turney, C.S.M., Johnson, F., 2022. Unprecedented high northern Australian streamflow linked to an intensification of the Indo-Australian monsoon. Water Resour. Res. 58 (3), e2021WR030881.
Jaffrés, J.B.D., Cuff, B., Cuff, C., Faichney, I., Knott, M., Rasmussen, C., 2021. Hydrological characteristics of Australia: relationship between surface flow, climate and intrinsic catchment properties. J. Hydrol. 603, 126911.
Jaffrés, J.B.D., Cuff, B., Cuff, C., Knott, M., Rasmussen, C., 2022. Hydrological characteristics of Australia: national catchment classification and regional relationships. J. Hydrol. 612, 127969.
Jaffrés, J.B.D., Cuff, C., Rasmussen, C., Hesson, A.S., 2018. Teleconnection of atmospheric and oceanic climate anomalies with Australian weather patterns: a review of data availability. Earth Sci. Rev. 176, 117–146.
Jeffrey, S.J., Carter, J.O., Moodie, K.B., Beswick, A.R., 2001. Using spatial interpolation to construct a comprehensive archive of Australian climate data. Environ. Model. Software 16 (4), 309–330.
Kuentz, A., Arheimer, B., Hundecha, Y., Wagener, T., 2017. Understanding hydrologic variability across Europe through catchment classification. Hydrol. Earth Syst. Sci. 21 (6), 2863–2879.
Laaha, G., Blöschl, G., 2006. A comparison of low flow regionalisation methods—catchment grouping. J. Hydrol. 323 (1–4), 193–214.
Lewis, S., Packett, B., Dougall, C., Brodie, J., Bartley, R., Silburn, M., 2015. Fitzroy sediment story. A report for the Fitzroy Basin Association, No. 15/74. James Cook University, Townsville, p. 38.
Li, C., Zwiers, F., Zhang, X., Chen, G., Lu, J., Li, G., Norris, J., Tan, Y., Sun, Y., Liu, M., 2019. Larger increases in more extreme local precipitation events as climate warms. Geophys. Res. Lett. 46 (12), 6885–6891.
Liu, B., Wang, D., Fu, S., Cao, W., 2017. Estimation of peak flow rates for small drainage areas. Water Resour. Manag. 31 (5), 1635–1647.
Risbey, J.S., Pook, M.J., McIntosh, P.C., Wheeler, M.C., Hendon, H.H., 2009. On the remote drivers of rainfall variability in Australia. Mon. Weather Rev. 137 (10), 3233–3253.
Robinson, J.S., Sivapalan, M., 1997. Temporal scales and hydrological regimes: implications for flood frequency scaling. Water Resour. Res. 33 (12), 2981–2999.
Sharma, A., Wasko, C., Lettenmaier, D.P., 2018. If precipitation extremes are increasing, why aren't floods? Water Resour. Res. 54 (11), 8545–8551.
Smith, J.A., 1992. Representation of basin scale in flood peak distributions. Water Resour. Res. 28 (11), 2993–2999.
Visser, J.B., Wasko, C., Sharma, A., Nathan, R., 2023. Changing storm temporal patterns with increasing temperatures across Australia. J. Clim. 36 (18), 6247–6259.
Wasko, C., Nathan, R., Stein, L., O'Shea, D., 2021. Evidence of shorter more extreme rainfalls and increased flood variability under climate change. J. Hydrol. 603, 126994.
Wasko, C., Westra, S., Nathan, R., Pepler, A., Raupach, T.H., Dowdy, A., Johnson, F., Ho, M., McInnes, K.L., Jakob, D., Evans, J., Villarini, G., Fowler, H.J., 2024. A systematic review of climate change science relevant to Australian design flood estimation. Hydrol. Earth Syst. Sci. 28 (5), 1251–1285.
Webster, I.T., Ford, P.W., 2010. Delivery, deposition and redistribution of fine sediments within macrotidal Fitzroy Estuary/Keppel Bay: Southern Great Barrier Reef, Australia. Continental Shelf Res. 30 (7), 793–805.